LETTERS TO THE EDITOR

The Letters to the Editor section is divided into four categories entitled Communications, Notes, Comments, and Errata. Communications are limited to three and one half journal pages, and Notes, Comments, and Errata are limited to one and three-fourths journal pages as described in the Announcement in the 1 January 1997 issue.

COMMUNICATIONS

Caging phenomena in reactions: Femtosecond observation of coherent, collisional confinement

C. Wan, M. Gupta, J. S. Baskin, Z. H. Kim, and A. H. Zewail
Arthur Amos Noyes Laboratory of Chemical Physics, California Institute of Technology, Pasadena, California 91125

(Received 15 November 1996; accepted 6 January 1997)

We report striking observations of coherent caging of iodine, above the *B* state dissociation threshold, by single collisions with rare gas atoms at room-temperature. Despite the random nature of the solute–solvent interaction, the caged population retains coherence of the initially prepared unbound wave packet. We discuss some new concepts regarding dynamical coherent caging and the one-atom cage effect. © *1997 American Institute of Physics.* [S0021-9606(97)03910-X]

I. INTRODUCTION

Since 1934, the caging phenomenon has become a fundamental concept in the description of reaction mechanisms. The general picture given in textbooks invokes the formation of the two reactants, e.g., by diffusion, within a ''solvent cage'' and the subsequent reaction of the ''encounter pair'' within the cage. In the classical experiments on photodissociation and caging of iodine in solution, the mechanism depicted[1] is that of a separation of the atoms upon dissociation, the stopping of the atoms when they separate to ''infinite'' distance R_∞ by losing the available energy to the solvent, and the recombination in the solvent cage after transition to the ground state surface near R_∞. The recombination is accomplished by a diffusive motion of the pair and multiple collisions within the cage.[2] The first picosecond study[3] in solution has shown that the collision-induced predissociation occurs in <10 ps and that ''caging'' can be observed. Since then this system has been examined in all phases by excitation to either the *B* or *A* state.[4]

In van der Waals complexes, the one-atom cage effect has been observed for I_2-Ar.[5,6] The mechanism has attracted many theoretical and experimental studies with attention given to the kinematics of the half collision and to the nature of the electronic states involved. Originally,[5] it was proposed that caging of the two iodine atoms occurs as a result of an impulsive transfer of energy to argon. Subsequently,[6] the notion of a nonadibatic coupling between two surfaces was introduced. Recently, studies[7] of fluorescence from continuum excitation have shown consistency with the linear isomer[7,8] model, which suggests its involvement in the one-atom cage effect on the *B* state.

In this communication, we report direct femtosecond (fs) studies of caging under bimolecular, single-collision conditions. We focus on the prototype reaction of iodine, which started all studies of the phenomena, with the solvent being rare gases at different densities. By preparing a wave packet above the dissociation limit of the *B* state, we observe striking results: collisional confinement with the atoms not reversing their momentum, caging at shorter internuclear separations, and caging coherently. The observations reported here indicate that a solvent structure is not the only critical factor in *bimolecular* solvent caging, and the mechanism can be described as a single collision effect. For this bimolecular caging, we also show that the proposed mechanism of surface hopping in the so-called one-atom cage effect is not valid. This is shown by preparing an ''oriented'' wave packet and observing in real time its polarized evolution.

II. EXPERIMENT AND RESULTS

Femtosecond pulses (60 fs, 770–830 nm, 700 μJ) were generated using a Ti:sapphire laser. A portion of the fundamental pulse was doubled to generate a probe beam pulse (385–415 nm, attenuated to 5 μJ). The remaining fundamental pulse ($\sim$600 μJ) was then sent into an optical parametric amplifier to generate an IR pulse which was subsequently mixed with a residual fundamental pulse to generate the pump beam ($\sim$496 nm, 5–10 μJ). Both pulses were passed through polarizers and the polarization of the probe was accurately controlled. The probe beam was delayed using a computer controlled actuator before being recombined with the pump beam at a dichroic mirror. The pump and probe beams were passed through the sample cell and fluorescence was collected perpendicular to the direction of beam propagation and detected by a PMT. The high-pressure sample cell has been described previously[9] and experimental details will be provided in a full account of this work.

The pump pulse prepares wave packets at energies above the *B* state dissociation level. The probe beam excites molecules to the ion pair states which then fluoresce. Transients were recorded at a variety of rare gas pressures. Figure 1 shows sample transients in low pressures of solvent with pump and probe polarization forming an angle of 54.7°. At 0 bar, there is a single strong peak, which results from the wave packet passing through the probe window(s) once be-

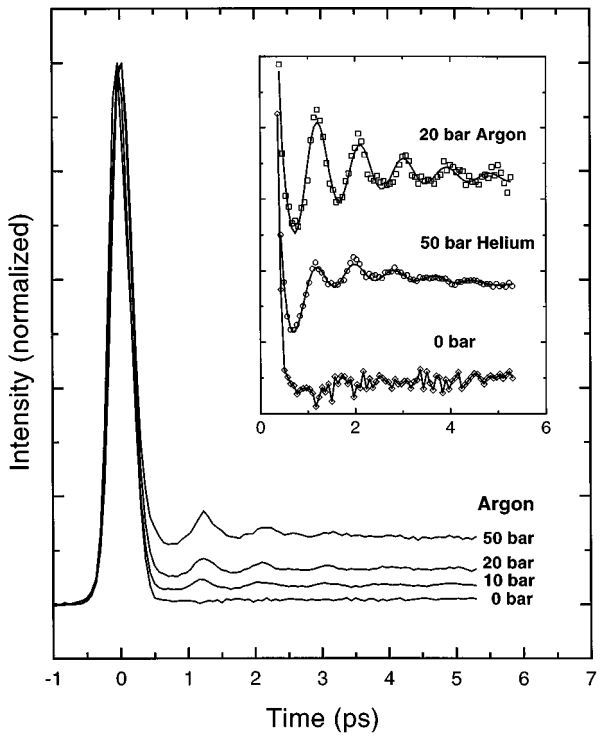

FIG. 1. Transients with $\lambda_{pump}=496$ nm and $\lambda_{probe}=389$ nm at argon pressures of 0, 10, 20, and 50 bar normalized to their peak heights. Inset shows expanded transients for 50 bar helium, 20 bar argon, and 0 bar, with exponentially damped single cosine fits for the oscillations (50 and 20 bar). The argon transients are expanded by a factor of ~6 and the helium transient ($\lambda_{pump}=498$ nm, $\lambda_{probe}=395$ nm) is arbitrarily scaled.

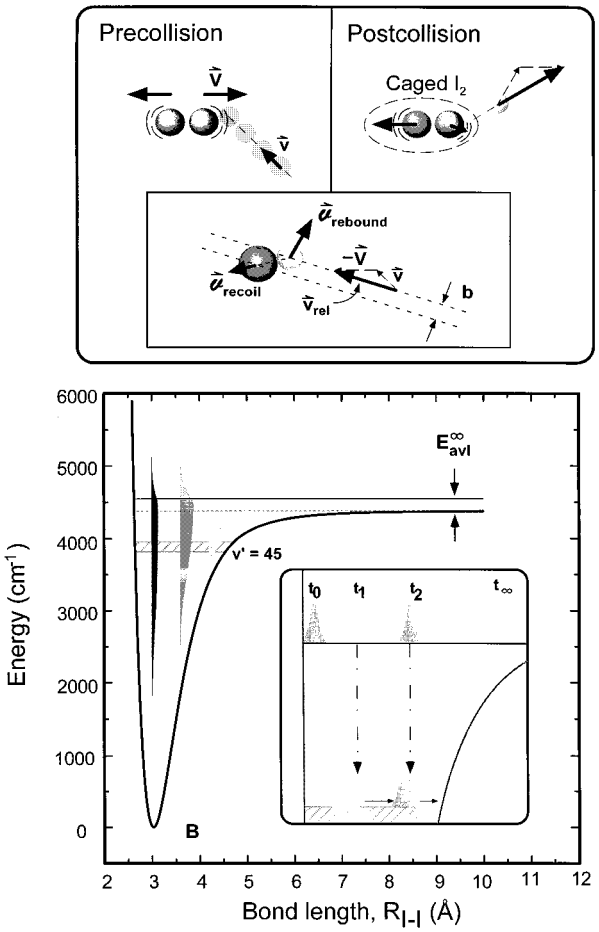

FIG. 2. Single Collisional Caging. (Top) The pertinent I–Ar collision parameters are shown: $\vec{V}$ and $\vec{v}$ are the initial I atom velocity and initial argon velocity, respectively, $\vec{v}_{rel}$ is the relative velocity, and b is the impact parameter. Note that, in the precollision iodine-atom rest frame shown in the box, $\vec{v}_{rel}$ is the initial velocity of the argon. In the same frame $\vec{\omega}$ is the postcollision velocity for recoil of $I(\vec{\omega}_{recoil})$ and for rebound of argon $(\vec{\omega}_{rebound})$. To obtain the postcollision velocities in the lab frame (upper right), $\vec{V}$ must be added to these, as shown for argon. For simplicity, the collision shown is one in which all atoms move in a single plane. (Bottom) iodine potential energy surfaces showing calculated final B state energy distributions (plotted in the well) of I_2 after a single collision with argon, as a function of bond length (3, 3.6, 4.2 Å). The hatched area represents the energy accessed by the Franck–Condon probe window. Inset shows schematically the position of the initial wave packet at different times $(t_0,\ t_1,\ t_2, \ldots)$ and the populations caged to the energy specified (see text) by collisions at times t_1 and t_2; the horizontal arrows indicate the direction of motion of the caged wave packets.

fore dissociating, with very little residual signal. When argon is added, the greatly enhanced residual signal after the initial peak comes from molecules which are caged into the B state. The signal from the caged molecules increases approximately linearly with pressure. The inset shows an expanded view of the signal for pure I_2 (0 bar), I_2 in argon (20 bar) and I_2 in helium (50 bar). The oscillations in the transient are fit to an exponentially damped single cosine to determine their period as described below. The transients in helium are similar to those in argon but with a smaller signal at equal pressures. The behaviors with polarization of the pump and probe pulses are discussed below.

III. DISCUSSION

A. Dynamics of single-collision, coherent caging

The oscillations in the transients of Fig. 1 indicate that the caged molecules are undergoing coherent motion, even though the caging results from a random collision at room temperature. When a collision between a rare gas atom and an iodine molecule causes caging, the molecule loses kinetic energy while retaining its I–I distance (R_{I-I}). In Fig. 2 , we show the kinematics of a single bimolecular collision (top) and the energetics and potential energy (bottom). As discussed below, the initial wave packet (bottom inset) at t_0 evolves with time $(t_1,\ t_2, \ldots)$ and caging leads to the energy distributions shown to span from above the B state to far down in the potential well (bottom figure). The probe window selects the cage population at a particular energy, e.g., near $v_B=45$.

Kinematic considerations show that the newly caged molecule continues to stretch, although at a slower rate than the original wave packet. As more iodine are caged, all caged molecules which fall to the same B state vibrational level are approximately in phase, as illustrated in Fig. 2 (bottom, inset). At the outer turning point of the B state, the dissociating molecules continue to separate, while the caged ones begin to oscillate in the bound B state.[10] In this picture, coherence will only be retained for molecules caged to their final ob-

served level in synchrony with the passage of the dissociating wave packet. Note that the coherence of the caged iodine is a remnant of the coherence of the initial wave packet.

The energy of a caged molecule depends on the impact parameter for collision, the velocities (speed and angle of collision), and the solvent (Fig. 2, top). Since each range of vibrational levels has a particular period of oscillation, the vibrational energy of the caged I_2 which gives rise to the observed signal can be determined from the oscillation period. For example, at a probe wavelength of 396 nm, the period was 868 fs in 10 bar argon. This period was found to be roughly independent of solvent pressure (below 50 bar). In helium, a similar period was observed. For $J=51$ (the peak of the ground state angular momentum distribution), this period corresponds to molecules centered at the $v_B=45$ vibrational level in the B state. Coherent caging to this vibrational level must occur before the iodine atoms exceed a separation of ~4.6 Å, the outer turning point of the vibrational motion. The caging *does not* occur far into the asymptotic region of the potential as is often believed. Simple calculations on the B state potential energy surface show that the wave packet reaches 4.6 Å in under 250 fs, and, therefore, coherent caging must occur within this time frame.

At the lowest pressures used in this study, the probability of a single iodine suffering two or more collisions with the solvent within this short time compared to the probability of one collision is very small (~1% for 10 bar argon, where the time between collisions is ~16 ps). Moreover, the intensity of the signal from caged iodine increases linearly with rare gas density, consistent with caging by a single collision mechanism within the fs time window for coherent caging. Furthermore, at the pressures used, when the I_2 are prepared high ($v_B>53$) within the B state, we do not observe the period seen under caging conditions. This indicates that even if dissociating I_2 were to collide more than once in the required time period, any I_2 which are left at a high energy after the first collision cannot make significant contributions to the coherent signal. Therefore, we conclude that the coherent signal results from a single collision with one solvent atom.

In Fig. 2 (bottom) we show theoretical calculations of the distributions of final I_2 internal energy, for impacts at three specific bond lengths. The calculations were for the case of randomly distributed, single, hard sphere collisions of I_2 ($J=0$) with a Maxwell–Boltzmann distribution of argon atoms. The distributions are very broad due to the random nature of the collision process, so if all the caged I_2 molecules were probed simultaneously, the incommensurate oscillations from different v_B levels would interfere in the signal, and the coherence would most likely not be observable. That we are able to observe the coherence cleanly derives from the circumstance that only a small range of vibrational levels are probed. Calculations show that the Franck–Condon factors for the $E \leftarrow B$ probe transition at $\lambda=396$ nm are strongly peaked in the vicinity of the transition from $v_B=44$–46 to $v_E=35$–37.[11] At a shorter probe wavelength, 389 nm, the oscillations have a longer period of 907 fs, corresponding to $v_B \sim 46$. When tuned to the red, 408.5 nm, the period changed to 703 fs, $v_B=40$–41. These changes are consistent with the expected wavelength dependence of the Franck–Condon probe window. Thus, although the distribution of caged molecules does not change, different segments of the population can be probed selectively.

Averaged over the trajectory of the dissociating wave packet, the hard sphere *single* collision calculations show that ~0.1% of excited I_2 are caged to v_B within the range 44–46 both in 50 bar helium and in 10 bar argon; the total caging is 40 and 18 times larger, respectively. For argon, 90% of the contribution to observed caging comes from bond lengths within the range 2.67–4.25 Å. For helium to cage iodine to these levels, the iodine atoms must have a high kinetic energy and must therefore be even closer to their equilibrium separation (maximum kinetic energy), with 90% of the contribution between 2.8 and 3.5 Å, corresponding to a time window for collision of only 50 fs. The distributions of velocity and impact parameter of the colliding rare gas atom that contribute to caging are also more restricted for helium than for argon, due to helium's lighter mass.

B. Mechanism of the one-atom cage effect

The single bimolecular collision finding discussed above has direct implications to the mechanism of the cage effect observed in the half-collision studies of I_2–Ar van der Waals complexes.[5,15] Following the original publication of the one-atom cage effect,[5] two possible mechanisms have been suggested: (1) a purely collisional transfer of energy from the iodine to the rare gas or (2) an electronic coupling of the iodine $^1\Pi_{1_u}$ and B states, in which the molecule is first excited to the purely repulsive $^1\Pi_{1_u}$ state and then nonadiabatically crosses to a bound level of the B state; above the B state excitation leads to wave packets on both the B state (60%) and the $^1\Pi_{1_u}$ state (40%).[14] As mentioned in the introduction, studies[7] of fluorescence for continuum excitation is consistent with a linear isomer structure of I_2–Ar[7,8] which may be responsible for the caging on the B state; see also MD simulations.[12]

This question of the nonadiabatic coupling mechanism[6] can be elucidated by studies of the evolution of the wave packet fs polarization anisotropy:[16] $r(t) = (I_\parallel - I_\perp)/(I_\parallel + 2I_\perp)$, where $I_\parallel$ and $I_\perp$ are transients measured with the probe polarization parallel and perpendicular, respectively, to the pump polarization. The $B(^3\Pi_{0^+_u})$ state has a total angular momentum about the internuclear axis, $\Omega=0$. The X, $^1\Pi_{1_u}$, and E (0^+_g) states have $\Omega=0$, 1, and 0, respectively.[17] Transitions for which $\Delta\Omega=0$ are termed parallel transitions because the transition dipole is parallel to the internuclear axis; likewise, if $\Delta\Omega=1$, the transition is termed perpendicular.[18] Therefore, the $B \leftarrow X$ pump transition is a parallel transition, whereas the $^1\Pi_{1_u} \leftarrow X$ dipole is perpendicular. The $E \leftarrow B$ probe transition dipole is parallel.

We have measured the anisotropy when wave packets were prepared *above* and *below* the B state dissociation threshold (Fig. 3). For excitation to the B state near $v_B=45$, the polarization anisotropy $r(t)$ is very similar to

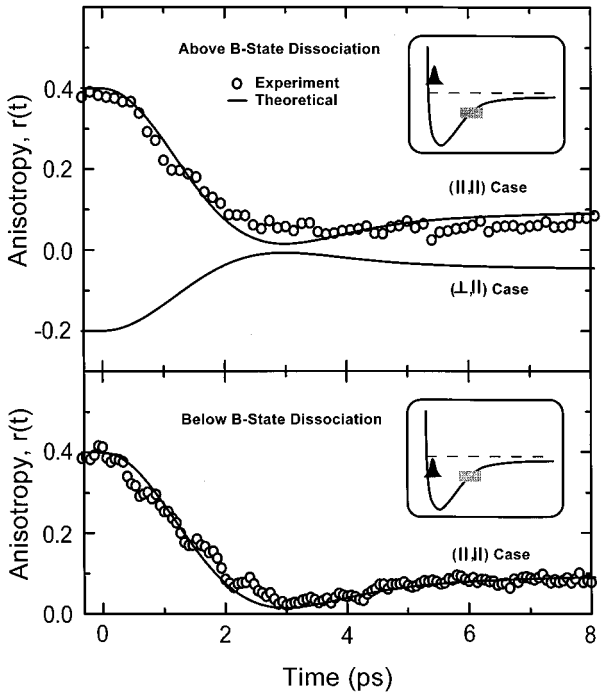

FIG. 3. (Bottom) measured anisotropy (open circles) (λ_{pump}=513 nm, λ_{probe}=395 nm) in 20 bar argon with excitation *below* the *B* state dissociation threshold. (Top) measured anisotropy (open circles) (λ_{pump}=495 nm, λ_{probe}=395 nm) in 20 bar argon with excitation *above* the *B* state. Solid lines represent theoretical anisotropies for two different dipole transition sequences, calculated for direct excitation to v_B=45 at 0 bar (see text). Insets depict the position of the wave packet and window of probing for the two cases studied.

that predicted theoretically for a ||,|| dipole sequence (see Fig. 3, bottom) as expected for probing to the *E* state; the initial anisotropy is in accord with theory and the transient behavior is entirely consistent with theory.[16] When a packet is prepared above the *B* state and collisionally cages into the *B* state, where it is probed via the same probe transition, the anisotropy (Fig. 3) is very similar to that of the wave packet originally prepared within the *B* state, and therefore also consistent with a ||,|| sequence.

If I_2 were first excited onto the $^1\Pi_{1_u}$ state and then crossed to the *B* state before being probed to the *E* state, the anisotropy would reveal a ⊥, ∥ pump–probe sequence. The theoretical calculation with $r(0)=-0.2$ in Fig. 3 corresponds to this dipole case ($\Omega=1\leftarrow\Omega=0$, $\Omega=0\leftarrow\Omega=0$). and contrasts starkly with the observation. Therefore, the caging dynamics occur on the *B* state, contrary to the $^1\Pi_{1_u}/B$ nonadiabatic surface hopping mechanism.

IV. CONCLUSION

In conclusion, from the results presented here for *bimolecular* caging, we have discussed the following dynamical picture: instead of regarding the solvent as a barrier to dissociation, the solvent is treated as an active, incoming collider. The solute atoms do not separate to ''infinite'' distances, but are instead caged very rapidly (fs) and coherently by a single collision with the solvent. Thus, the key here is the fs time scale of the caging and the caging while atoms are in proximity (large kinetic energy). For the mechanism, we have presented evidence that electronic surface hopping does not play a role in the caging dynamics of the bimolecular encounter. The caged molecules retain the coherence of the initial wave packet and are selectively observed by the probe window. Extensions of this work to higher pressures, different wavelengths, and different solvents, as well as a full theoretical treatment, will be given in a complete account.

[1] J. Franck and E. Rabinowitch, Trans. Faraday Soc. **30**, 120 (1934); E. Rabinowitch and W. C. Wood, Trans. Faraday Soc. **32**, 1381 (1936).
[2] L. F. Meadows and R. M. Noyes, J. Amer. Chem. Soc. **82**, 1872 (1960); J. Zimmerman and R. M. Noyes, J. Chem. Phys. **18**, 658 (1950); J. Schroeder and J. Troe, Annu. Rev. Phys. Chem. **38**, 163 (1987).
[3] T. J. Chuang, G. W. Hoffman, and K. B. Eisenthal, Chem. Phys. Lett. **25**, 201 (1974).
[4] For recent reviews see: A. Harris, J. K. Brown and C. B. Harris, Annu. Rev. Phys. Chem. **39**, 341 (1988); C. Lienau and A. H. Zewail, J. Phys. Chem. **100**, 18 629 (1996), and references therein.
[5] J. J. Valentini and J. B. Cross, J. Chem. Phys. **77**, 572 (1982).
[6] J. A. Beswick, R. Monot, J.-M. Philippoz, and H. van den Bergh, J. Chem. Phys. **86**, 3965 (1987).
[7] M. L. Burke and W. Klemperer, J. Chem. Phys. **98**, 1797 (1993).
[8] M. C. R. Cockett, D. A. Beattie, R. J. Donovan, and K. P. Lawley, Chem. Phys. Lett. **259**, 554 (1996).
[9] A. Materny, C. Lienau, and A. H. Zewail, J. Phys. Chem. **100**, 18 650 (1996); Q. Liu, C. Wan, and A. H. Zewail, *ibid.*, 18 666 (1996).
[10] R. M. Bowman, M. Dantus, and A. H. Zewail, Chem. Phys. Lett. **161**, 297 (1989); M. Gruebele and A. H. Zewail, J. Chem. Phys. **98**, 883 (1993).
[11] Franck–Condon factors were calculated by the Numerov method [see B. R. Johnson, J. Chem. Phys. **67**, 4086 (1977)], using a *B* state potential (see Refs. 10, 12, 13) and an *E* state Morse potential fit to RKR points from Ref. 13.
[12] H. Schröder and H. Gabriel, J. Chem. Phys. **104**, 587 (1996), and references therein.
[13] For the *B* state, see S. Gerstenkorn and P. Luc, J. Physique **46**, 867 (1985). For the *E* state, see J. C. D. Brand, A. R. Hoy, A. K. Kalkar, and A. B. Yamashita, J. Mol. Spectrosc. **95**, 350 (1982). See also Ref. 14.
[14] J. Tellinghuisen, J. Chem. Phys. **76**, 4736 (1982).
[15] K. L. Saenger, G. M. McClelland, and D. R. Herschbach, J. Phys. Chem. **85**, 3333 (1981).
[16] P. M. Felker and A. H. Zewail, J. Chem. Phys. **86**, 2460 (1987); J. S. Baskin and A. H. Zewail, J. Phys. Chem. **98**, 3337 (1994).
[17] See R. S. Mulliken, J. Chem. Phys. **55**, 288 (1971), and Ref. 14.
[18] R. S. Mulliken, Phys. Rev. **36**, 699, 1440 (1930).